

PACS numbers: 42.55.Lt; 33.20.Tp; 52.80.–s
DOI: 10.1070/QE2012v042n01ABEH014693

Two-dimensional model of an active medium of a fast-flow CO laser with state-to-state vibrational kinetics

V.A. Gurashvili, E.M. Zanozina, I.V. Kochetov, A.K. Kurnosov, D.I. Spitsin

Abstract. **A two-dimensional numerical model of the active medium of a fast-flow electron-beam-controlled CO laser, taking the latest achievements of state-to-state vibrational kinetics into account, is developed. The model includes detailed kinetics and spatial description of non-self-sustained discharge in the gas flow. Using this model the basic characteristics of two schemes of a gas-flow CO laser with subsonic and supersonic flow of the gas mixture are compared.**

Keywords: *CO laser, two-dimensional numerical model, non-self-sustained discharge, vibrational kinetics, energy balance.*

1. Introduction

The CO laser holds a high position among cw gas lasers, and numerous papers are devoted to theoretical studies of kinetic processes in its active medium [1–4]. Originally the analytical [5–7] and simplified [8] models of the vibrational kinetics were developed, which allowed estimation of the characteristics of CO lasers. With the appearance of high-efficiency computation technique, besides the analytical models, numerical models of the active medium appeared that allow simultaneous solution of one-dimensional equations of gas dynamics, kinetic equations for vibrational energy levels, and Boltzmann equations for the electron energy distribution function (EEDF) [9, 10], as well as calculation of the radiation intensity in the diffraction approximation [11].

The necessity for modelling high-power gas lasers is still urgent. In this case an important problem is the appropriate account for spatial inhomogeneity of the excitation power density and the active medium heating, arising from non-uniform ionisation of the gas by fast electrons and boundary effects. Spatial inhomogeneities of the discharge may lead to worsening the quality of laser radiation, the characteristic of primary importance in laser design.

In the present paper we describe a two-dimensional model that accounts for the spatial inhomogeneities of the active medium ionisation, of the electric field and of the gas flow. The model includes detailed description of vibrational kinetics, based on the results of semiclassical calculations of the rate constants for different processes, including multiquantum ones.

2. Numerical model

The numerical model is based on the earlier one that includes the equations of gas dynamics in the thin-flux-tube approximation, the equations of electrodynamics, the equations for concentration of electrons, and the equations of vibrational kinetics in the approximation of the analytical theory [12, 13]. The new model is completed with the Boltzmann equation for EEDF in the two-term approximation with the collisions between electrons and vibrationally excited molecules taken into account, and with the equations of state-to-state vibrational kinetics. The present model allows the most complete description of the processes of the vibrational energy acquisition and relaxation at any degree of excitation, including very high vibrational energy levels.

To calculate the rate of ionisation of the CO-laser active medium by a beam of fast electrons, we used the Monte Carlo method in the approximation of 'effective collisions' [14, 15] that correctly takes into account the specific features of the gas discharge chamber (GDC) construction and the spatial inhomogeneity of the current density distribution in the electron beam.

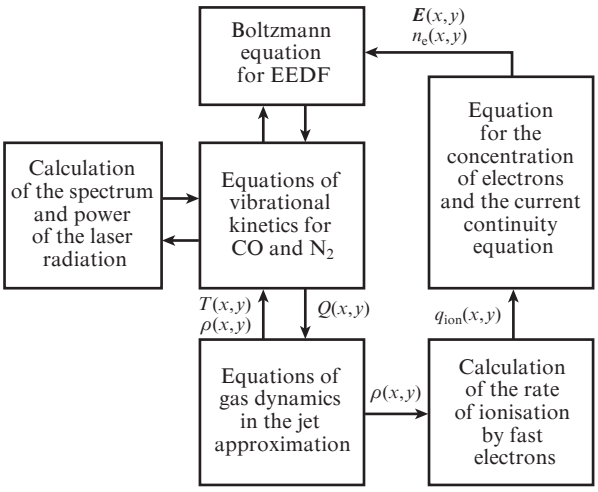

Figure 1. Block diagram of the two-dimensional numerical model of the active medium in a fast-flow CO-laser:
$\boldsymbol{E}(x,y)$ is the electric field strength; $n_e(x,y)$ is the concentration of electrons; $T(x,y)$ is the translational gas temperature; $\rho(x,y)$ is the density of the mixture; $Q(x,y)$ is the specific power of gas heating; $q_{ion}(x,y)$ is the rate of the active medium ionisation.

V.A. Gurashvili, E.M. Zanozina, I.V. Kochetov, A.K. Kurnosov, D.I. Spitsin State Research Center of Russian Federation 'Troitsk Institute for Innovation and Fusion Research', ul. Pushkovykh, vladenie 12, 142190 Troitsk, Moscow region, Russia;
e-mail: kochet@triniti.ru

Received 11 July 2011; revision received 17 October 2011
Kvantovaya Elektronika **42** (1) 21–26 (2012)
Translated by V.L. Derbov

The model comprises several computational units describing different physical processes. The equations that enter these units are solved sequentially and the values of parameters are exchanged between the units. The block diagram of the numerical model is presented in Fig. 1.

2.1. Gas dynamics calculation in the thin-flux-tube approximation

We consider a steady-state flow of the gas mixture in the discharge chamber, whose cross section may vary along the flow. In the vertical direction the flow is divided into thin (one-dimensional) flux tubes such that in a cross section of each individual flux tube the parameters of the flow are uniform and the velocity of the flow has a fixed direction.

In the equations of gas dynamics, alongside with the heating due to dissipation of vibrational energy, the direct heating of the gas in the discharge was taken into account. The direct heating is caused by the presence of elastic losses in the collisions of electrons with heavy particles and by the excitation of rotational states, whose energy quickly relaxes into heat. The results of the experimental studies of the fraction of the pump power that goes straight into heating of N_2 and $CO-N_2$ mixtures under discharge are presented in a number or papers. In nitrogen the experimentally measured fraction of power that goes directly into heat is in good agreement with the calculated one [16]. For $CO-N_2$ mixtures the difference between the results reported by different authors is very large, and the question is still far from clarity [16]. Determination of the pump power fraction, lost in such mixtures due to direct heating in a non-self-sustained discharge, by solving the Boltzmann equation for EEDF [17] yields strongly underestimated values, as compared with the results of the experiments [18–20]. Possible reasons of this fact were analysed in [16, 21]. In the present work we used the fraction of the pump power 15% (lost by direct heating), which is close to the experimental data, obtained under the conditions, typical for operation of electron-beam-controlled CO lasers [18–20]. This approach provides satisfactory agreement between theory and experiments aimed to determine the energy characteristics of CO lasers and the initial growth dynamics of the small-signal gain [22].

2.2. Equations of vibrational kinetics

We solved numerically the equations of the state-to-state vibrational kinetics for the molecules CO and N_2, which can be presented in a simplified form as

$$\frac{\mathrm{d}N_v}{\mathrm{d}x}V(x) = R_\mathrm{e} + R_\mathrm{VV} + R_\mathrm{VV'} + R_\mathrm{VT} + R_\mathrm{sp} + R_\mathrm{ind} + V(x)N_v\left(\frac{1}{p}\frac{\mathrm{d}p}{\mathrm{d}x} - \frac{1}{T}\frac{\mathrm{d}T}{\mathrm{d}x}\right). \quad (1)$$

The terms in the right-hand side of the equations describe the variation of the population N_v of the vibrational energy level with the number v, caused by the following processes: the collisions of molecules in different vibrational states with the electrons of plasma (excitation and de-excitation of vibrational states) and with each other (VV exchange), the exchange of vibrational energy between different molecules (VV′ exchange), the transfer of vibrational energy into translational one under collisions with atoms and molecules (VT relaxation), the spontaneous and induced emission, as well as the change in the pressure p and the temperature T in the gas flow; $V(x)$ is the velocity of the gas flow.

In the description of the vibrational energy exchange between the CO molecules we used physically justified and, up to date, the most complete set of VV-exchange rate constants, including those of both single-quantum and multi-quantum processes. The role of the latter becomes essential for high vibrational levels [23], which is of particular importance for modelling the characteristics of the active medium of a CO laser in the absence of radiation and under the oscillation at the transitions of the first vibrational overtone of the CO molecule [22]. The rate constants of the single-quantum VV exchange between the N_2 molecules, CO and N_2 molecules were chosen in correspondence with [24]. The rate constants of asymmetric VV exchange (two quanta for one) between highly excited and nonexcited CO molecules were taken from [23], and for the processes of asymmetric VV exchange between the CO and N_2 molecules from [24].

2.3. Boltzmann equation for EEDF

In the solution of the stationary Boltzmann equation for a spherically symmetric component of EEDF within the two-term approximation [25, 26] the excitation of molecular rotational energy levels of N_2 and CO was taken into account using the diffusion approximation [16]. The cross sections of scattering of electrons by nonexcited CO molecules were taken from [27–29] and for N_2 molecules from [30]. The cross sections for the resonance part of the vibrational excitation of CO molecule from the ground state, taken from [29], were multiplied by 1.3 following the recommendations of [28, 31]. The collisions of the electrons with vibrationally excited CO molecules were taken into account. To determine the cross sections for the collisions of the second kind we used the principle of detailed balance. The interaction of electrons with vibrationally-excited molecules has different character depending on the energy level number v [32]. For $v \leqslant 9$ the scattering occurs mainly via the state of a short-lived negative ion and possesses a large resonance cross section. For $v > 9$ the potential scattering becomes essential, whose cross section grows monotonically with the energy level number, attaining $\sim 10^{-16}$ cm^2 at $v \geqslant 30$ [33]. Considering the collision of electrons with the CO molecules, occupying high ($v > 10$) vibrational energy levels, we took the processes of potential interaction into account.

The numerical algorithm for solving the Boltzmann equation for EEDF is described in [34]. The differential equation was replaced with a finite-difference scheme, defined on the energy-uniform mesh. The resulting set of linear equations was solved using the sweep method followed by iterations for the right-hand sides of the equations.

2.4. Equation for electron concentration and current continuity equation

The distributions of the electric field strength $\boldsymbol{E}$ and the discharge current density $\boldsymbol{j}$ were calculated in the approximation of quasi-neutral plasma from the equation $\mathrm{div}\,\boldsymbol{j} = 0$ using a finite-difference scheme under the condition of total current conservation, where $\boldsymbol{j} = |e|\mu_\mathrm{e} n_\mathrm{e}\boldsymbol{E}$; $\boldsymbol{E} = -\mathrm{grad}\,\varphi$; e is the electron charge; μ_e and n_e are the mobility and concentration of electrons; φ is the field potential. The mobilities μ_e were determined using EEDF.

The balance equation for the concentration of electrons has the form

$$\rho v \frac{\mathrm{d}}{\mathrm{d}x}\left(\frac{n_e}{\rho}\right) = q(x,y) - \beta_e n_e^2, \tag{2}$$

where ρ is the density of the mixture; $q(x,y)$ is the distribution of the rate of electron–ion pair creation in the discharge gap under the action of an external source, calculated using the Monte Carlo method [14, 15]; β_e is the coefficient of electron–ion recombination. The values of β_e were obtained by approximating the experimental data, presented in [35].

2.5. Calculation of power and spectrum of laser radiation

To calculate the multiple-frequency radiation spectrum the following balance equations for photons in the cavity were used:

$$\frac{\mathrm{d}I_{v,j}}{\mathrm{d}t} = c(G_{v,j} - \Gamma)I_{v,j} + \frac{L\Omega}{4\pi}N_v A_v, \tag{3}$$

where $I_{v,j}$ is the intensity for the given vibrational–rotational transition; $G_{v,j}$ is the gain; j is the number of P-branch rotational components; c is the velocity of light; L is the cavity length; Ω is the outlet mirror aperture; Γ is the threshold gain for the given transition; A_v is the Einstein coefficient for the considered transition. Equations (3) were integrated using the explicit–implicit scheme [36] together with the rest equations for the active medium. Because of fast transition to quasi-stationary regime, the condition $G_{v,j} = \Gamma$ was satisfied almost in the entire lasing region, which demonstrates the applicability of the 'constant gain' method for the active medium of the CO laser [37].

This method implies a number of essential simplifications. The oscillation spectrum is calculated at each point independently, whereas in a real cavity the efficient 'mixing' of radiation between different regions of the gas flow is provided. Within the framework of this method the intensity variation along the cavity axis is also neglected. To verify the practical applicability of the method, the authors of [37] compared its results with those of a more precise one, based on the solution of a set of parabolic equations for the field in an unstable cavity. In the balance equation for photons the threshold gain was calculated using the formula

$$\Gamma = \frac{1}{2L_a}\left(2\ln\frac{1}{R_{\mathrm{refl}}}\right) + \ln M_r, \tag{4}$$

where R_{refl} is the effective reflection coefficient of the mirrors; L_a is the transverse size of the active medium with respect to the flow; M_r is the magnification coefficient of the cylindrical cavity. Under the conditions, typical for fast-flow CO lasers, it was found that the lasing power values, calculated using both methods, agree with good accuracy [11, 37].

The lasing spectrum, calculated using Eqns (3), contains 2–3 rotational components of the P branch at each vibrational transition, whereas in the diffraction model only one rotational component corresponds to each vibrational transition. However, as follows from the calculated results, the radiation power distributions, obtained using both methods, are rather close to each other. Moreover, at the cavity axis the diffraction model yields the same number of P-branch rotational components, as the method of 'constant amplification'.

3. Numerical implementation of the model

The model is realised using the FORTRAN programming language. In the zero-order approximation the temperature, velocity and density of the gas in each flux tube were taken equal to their values at the entrance of the GDC. The initial concentration n_e of electrons was taken equal to the small 'background' concentration. It was assumed that at the metallic cathode the potential $\varphi = -U$ (U being the voltage applied to the discharge gap), and at the metallic anode $\varphi = 0$. Along each flux tube the electron mobilities, previously calculated by solving the Boltzmann equation for EEDF, were specified, as well as the rate of ionisation of molecules and atoms by fast electrons.

The set of equations, described above, is solved using the iteration method. The main computation cycle includes the calculation of the concentration of electrons, the potential and strength of the electric field, and the discharge current density. The elliptic equation for the potential is approximated using the conservative (conserving the full current) finite-difference scheme, constructed on the orthogonal mesh. The kinetic equations for vibrational energy levels are integrated along each flux tube using the Gear method [38]. The resulting data arrays for the radiation power, heating power, and the populations of the vibrational states are returned to the main cycle of the program to perform the next iteration.

The exit from the iteration cycle is determined by the convergence of the temperature $T(x,y)$ in all nodes of the mesh with the prescribed accuracy. The PC time consumption per cycle depends on the number of thin flux tubes, e.g., for 10 flux tubes it was nearly 5 minutes. To provide the relative accuracy of 10^{-3} about five iterations were necessary.

4. Numerical modelling results and discussion

The model was used for comparative analysis of two schemes of an electron-beam-controlled CO laser, one with subsonic [39] and the other with supersonic [40] flow of the gas mixture. In the subsonic scheme the gas mixture is cooled in special cooling units before entering the GDC, while in the supersonic one the cooling is implemented via adiabatic expansion of the mixture in the supersonic jet.

The calculation was performed with the input parameters listed below. The present choice of the parameters provided nearly the same input energy for both schemes at the given voltage applied to the discharge gap. Note, that for the subsonic CO laser the input energy ~150 J g^{-1} is easily accessible, whereas for the supersonic CO laser this value is close to an extreme one because of the necessity to provide a large current density in the beam of fast electrons. For the subsonic CO laser the divergence of the gas dynamical tract along the flow was introduced to prevent transition into transonic regime under the considered conditions. The change in the voltage applied to the discharge gap led to the change in the reduced electric field strength E/N (N is the gas number density) in the centre of the discharge from 5 to 15 Td and to the growth of the specific input energy from 50 to 350 J g^{-1}.

Input parameters for calculation

	Subsonic laser	Supersonic laser
Gas mixture	$CO:N_2 = 1:9$	$CO:N_2 = 1:9$
Temperature/K	80	80
Pressure/Torr	45	45

Gas velocity/m s^{-1}. 90	640
Summary divergence angle of the jet/grad 6	0
Electron beam current density in the ionisation source/μA cm^{-2} 10	160

The results of numerical modelling show that the variations of temperature in the GDC along the flow are almost similar for the two lasers, while the gas density distributions are different. Figure 2 presents the gas density distribution in the discharge zone. It is seen that in the supersonic CO laser the variation of the gas density (at the input energy 150 J g^{-1}) does not exceed 6%, while in the subsonic laser (at the same input energy) the gas density decreases by 40%.

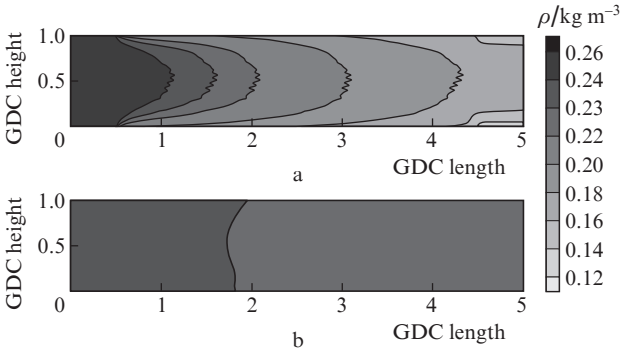

Figure 2. Distribution of the gas density in the discharge zone for the subsonic (a) and supersonic (b) CO lasers. The height and length of GDC are scaled to the channel height at the GDC entrance. The specific input energy is Q_{in} = 150 J g^{-1}.

Figure 3 shows the dependence of the specific input energy on the reduced electric field strength for the considered CO laser schemes. The specific input energy grows quadratically with the growth of E/N, virtually independently of the chosen scheme. To increase the specific input energy one needs higher values of E/N; however, in practice increasing E/N leads to discharge instability at $E/N \geqslant 15$ Td [41].

Figure 4 shows the calculated dependence of the specific extracted energy on the specific input energy for the subsonic and supersonic CO lasers. At the values of the specific input energy smaller than 200 J g^{-1} this dependence is close to linear.

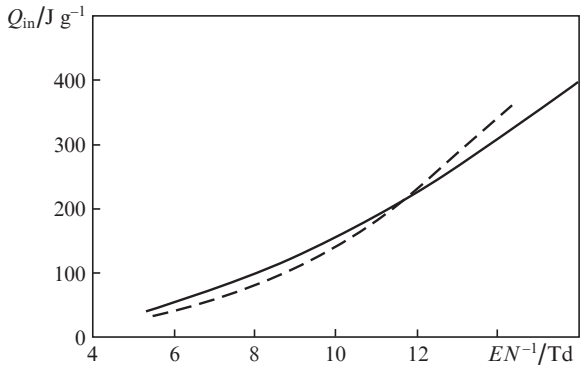

Figure 3. Dependences of specific input energy on E/N for supersonic (solid line) and subsonic (dashed line) CO laser schemes.

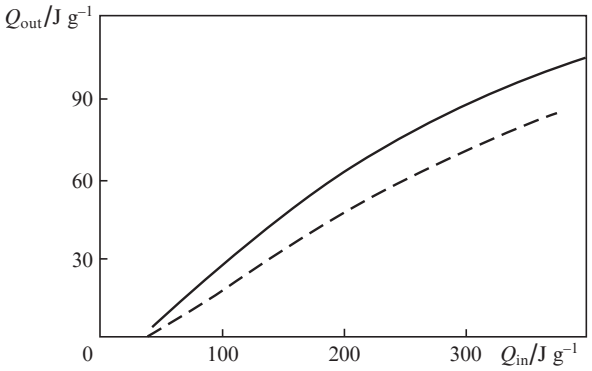

Figure 4. Specific extracted energy versus specific input energy for the supersonic (solid line) and subsonic (dashed line) schemes of the CO laser.

Figure 5 presents the efficiency of the CO lasers versus the reduced electric field strength E/N. It is seen that the value of E/N exists at which the efficiency is maximal. For the supersonic system the maximal efficiency (32%) is attained at E/N = 11 Td and for the subsonic one it is somewhat lower and equals 27% at E/N = 12.5 Td.

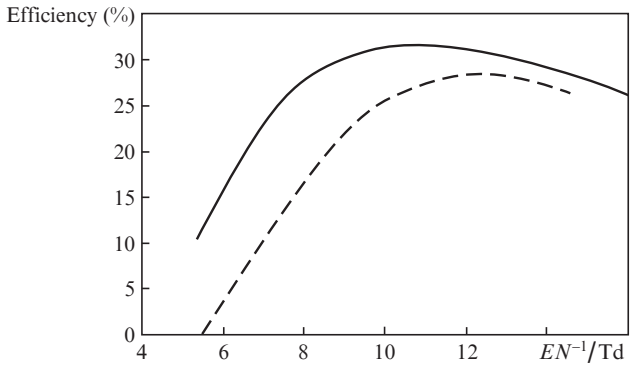

Figure 5. CO laser efficiency versus E/N for the supersonic (solid line) and subsonic (dashed line) schemes

To explain the dependence of the efficiency on E/N, it is necessary to analyse what happens with the energy deposited into the vibrational states of the molecules at the moment they leave the discharge zone. Figure 6 presents the fractions of the pump power $\kappa_i = W_i/W_{tot}$ (W_i being the power lost in the ith process, W_{tot} being the discharge power) deposited into the induced radiation of CO molecules and lost in different processes, namely, the removal of vibrationally excited CO and N_2 molecules from the active zone by the gas flow, the VV exchange, and the spontaneous emission. Note that in Fig. 6 the power fraction directly transformed into heat (15%) is not presented.

The maxima demonstrated by the dependences in Fig. 5 are caused by the increase in the discharge power fraction deposited into the vibrational states of N_2 molecules with the growth of E/N, as well as by the increasing vibrational energy, stored by N_2 and CO molecules, because of the growth of the gas translational temperature. As a consequence, the fraction of energy removed by the gas flow from the lasing zone ($\kappa_{N_2} + \kappa_{CO}$) increases.

Comparing the results of the efficiency calculations for two CO lasers considered, we may explain the efficiency decrease

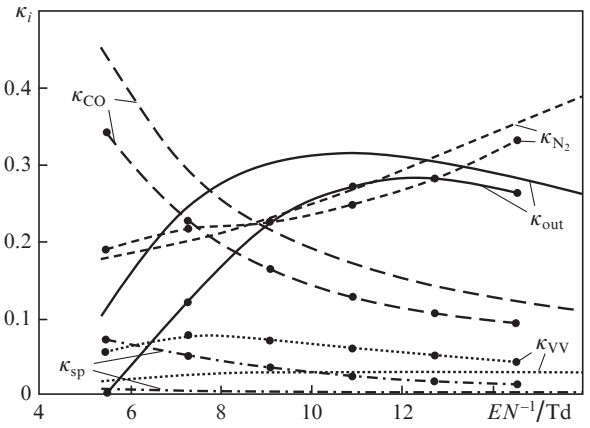

Figure 6. Power balance in the active medium at the exit of the discharge zone versus E/N: κ_{out}, κ_{CO}, κ_{N_2}, κ_{VV}, κ_{sp} are the pump power fractions deposited into laser radiation (efficiency), removed by the gas flow from the oscillation zone in the form of residual store of vibrational quanta of CO and N_2 molecules, transformed into heat in the VV exchange, and lost via spontaneous emission, respectively. The curves with points show the results of calculation for the subsonic CO laser, the curves without points relate to the supersonic one.

for the subsonic laser by greater energy losses via VV exchange and spontaneous emission, which is due to longer time spent by the working gas in the GDC. Note, that the energy fraction transformed into heat due to VT relaxation did not exceed a few thousandths per cent of the input energy for both schemes (for the considered composition of the gas mixture).

In the calculations of the laser radiation spectrum the number j of the rotational component of the P branch at each point of the aperture corresponded to the maximal gain coefficient. Therefore, the values of j changed along the flux tubes independently. Then the summation of the emission intensity for each vibrational–rotational transition over the flux tubes was performed. Figure 7 presents the vibrational–rotational spectra for both CO laser schemes, calculated in this way, at the same specific energy of excitation. The lasing spectrum for the subsonic scheme is shifted to the long-wave side due to significantly lower discharge power.

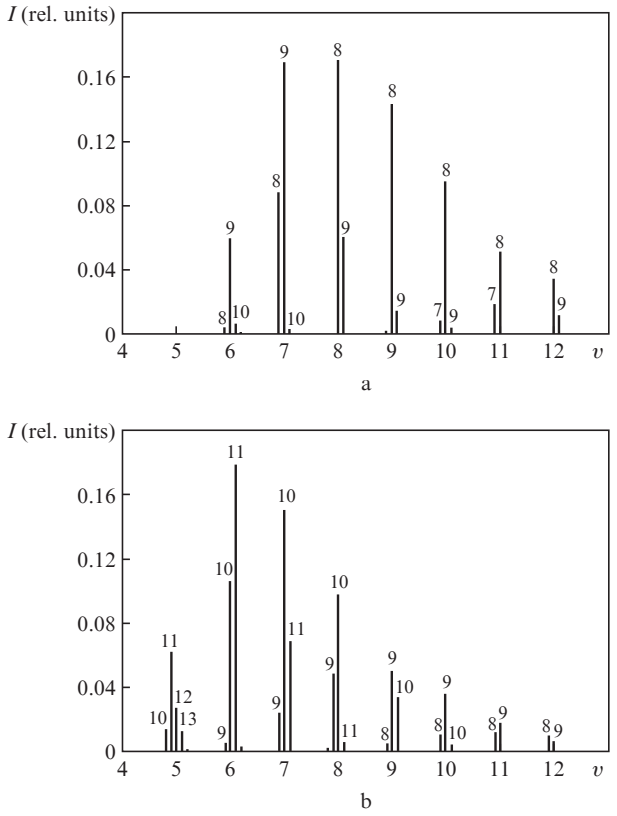

Figure 7. Vibrational–rotational emission spectrum of the subsonic (a) and supersonic (b) CO lasers. The numbers above the lines are the numbers j of the rotational components of the P branch, v is the number of the upper vibrational energy level for the corresponding transition, I is the intensity of the output radiation, $Q_{in} = -150$ J kg^{-1}.

5. Conclusions

The developed two-dimensional numerical model of the CO laser active medium allows the calculation of spatially non-uniform distributions of the pump power density and the laser radiation power density, the small-signal gains, the power of relaxation losses in the active medium, and the flow parameters. The model uses the most complete description of the energy exchange processes in the active medium, known to date.

The comparison of the gas density distribution in the two CO laser schemes under the considered conditions showed that in the supersonic CO laser the variation of density along the flow is 6.5 times smaller than in the subsonic one. The efficiency of the laser with the supersonic gas flow velocity is slightly greater than that of the subsonic one. Under the conditions of the calculations the short-wave edge of the emission spectrum of the supersonic CO laser corresponds to lower number of the vibrational transition, than in the case of subsonic laser.

References

1. Gordiets B.F., Osipov A.I., Stupochenko E.V., Shelepin L.A. *Usp. Fiz. Nauk*, **108**, 655 (1972) [*Sov. Phys. Usp.*, **15**, 759 (1973)].
2. Bubyakin G.B., Eletskii A.V., Populovskii V.F. *Usp. Fiz. Nauk*, **106**, 723 (1972).
3. Sobolev N.N., Sokovikov V.V. *Usp. Fiz. Nauk*, **110**, 191 (1973) [*Sov. Phys. Usp.*, **16**, 350 (1973)].
4. Konev Yu.B., Kochetov I.V., Pevgov V.G., Sharkov V.F. Preprint IAE No. 2821 (Moscow, 1977).
5. Zhdanok S.A., Napartovich A.P., Starostin A.N. *Zh. Eksp. Teor. Fiz.*, **76**, 130 (1979).
6. Gordiets B.F., Osipov A.I., Shelepin L.A. *Kineticheskiye protsessy v gazakh i molekulyarnye lasery* (Kinetic Processes in Gases and Molecular Lasers) (Moscow: Nauka, 1980).
7. Napartovich A.P., Novobrantsev I.V., Starostin A.N. *Kvantovaya Elektron.*, **4**, 2125 (1977) [*Sov. J. Quantum Electron*, **7**, 1216 (1977)].
8. Berdyshev A.V., Kochetov I.V., Napartovich A.P. *Khim. Fiz.*, **7**, 470 (1988).
9. Gurashvili V.A., Dem'yanov A.V., Zhdanok S.A., et al. *Inzhenerno-fiz. Zh.*, **55**, 37 (1988) [*J. Eng. Phys. Thermophys.*, **55** (1), 726 (1988)].
10. Araslanov Sh.F., Safiullin R.K. *Kvantovaya Elektron.*, **31**, 697 (2001) [*Quantum Electron.*, **31**, 697 (2001)].
11. Elkin N.N., Kochetov I.V., Kurnosov A.K., Napartovich A.P. Preprint IAE-5274/11 (Moscow, 1990).
12. Napartovich A.P., in *Gas Lasers – Recent Developments and Future Prospects (Nato ASI Series)* (Dordrecht–Boston–London: Kluwer Acad. Publ., 1995) Vol. 10, p. 11.
13. Napartovich A.P., Gurashvili V.A., Kochetov I.V., et al. *Proc. SPIE Int. Soc. Opt. Eng.*, **2702**, 420 (1996).
14. Dyatko N.A., Zanozina E.M., Kochetov I.V., Spitsyn D.I. Preprint TRINITI No. 146 (Troitsk, 2011).

15. Gurashvili V.A., Dzhigaylo I.D., Dyatko N.A., et al. *Fiz. Plazmy*, **38**, 52 (2012).
16. Deryugin A.A., Kochetov I.V., Loboyko A.I., et al. *Fiz. Plazmy*, **14**, 340 (1988) [*Sov. J. Plasma Phys.*, **14**, 200 (1988)].
17. Konev Yu.B., Kochetov I.V., Marchenko V.S., Pevgov V.G. *Kvantovaya Elektron*., **4**, 1359 (1977) [*Sov. J. Quantum Electron.*, **7**, 768 (1977)].
18. Basov N.G., Dolinina V.I., Zvorykina V.D., et al. Preprint FIAN No. 292 (Moscow, 1983).
19. Basov N.G., Kazakevich V.S., Kovsh I.B., Mikryukov A.N. *Kvantovaya Elektron*., **10**, 1049 (1983) [*Sov. J. Quantum Elelctron.*, **13**, 667 (1983)].
20. Aliev E.T., Basov N.G., Kovsh I.B., et al. *Kvantovaya Elektron*., **11**, 874 (1984) [*Sov. J. Quantum Electron*., **14**, 593 (1984)].
21. Konev Yu.B., Kurnosov A.K. *Teplofiz. Vys. Temp.*, **26**, 651 (1988).
22. Ionin A.A., Kurnosov A.K., Napartovich A.P., Seleznev L.V. *Laser Phys.*, **20**, 144 (2010).
23. Billing G.D., Coletti C., Kurnosov A.K., Napartovich A.P. *J. Phys. B: At. Mol. Opt. Phys*., **36**, 1175 (2003).
24. Cacciatore M., Kurnosov A.K., Napartovich A.P., Shnyrev S. *J. Phys. B: At. Mol. Opt. Phys.*, **37**, 3379 (2004).
25. Dyatko N.A., Kochetov I.V., Napartovich A.P., Taran M.D. Preprint IAE-3842/12 (Moscow, 1983).
26. Dyatko N.A., Kochetov I.V., Napatrovich A.P. *Fiz. Plazmy*, **18**, 888 (1992) [*Sov. J. Plasma Phys.*, **18**, 462 (1992)].
27. Land J.E. *J. Appl. Phys.*, **49**, 5716 (1978).
28. Haddad G.N., Milloy H.B. *Aust. J. Phys.*, **36**, 473 (1983).
29. Ehrhardt H., Langhans L., Linder F., Taylor H.S. *Phys. Rev.*, **173**, 222 (1968).
30. Phelps A.V., Pitchford L.C. *JILA Information Center Report No. 26* (Boulder, Colorado, University of Colorado, 1985).
31. Aleksandrov N.L., Kochetov I.V., Napartovich A.P. *Khim. Vys. Energ*., **20**, 291 (1986) [*High Energy Chem*., **20** (4), 223 (1986)].
32. Aleksandrov N.L., Konchakov A.M., Son E.E. *Zh. Tekh. Fiz.*, **49**, 1200 (1979) [*Sov. Phys. Tech. Phys.*, **24**, 664 (1979)].
33. Hake R.D., Phelps A.V. *Phys. Rev.*, **158**, 70 (1967).
34. Lacina W.B. *Theoretical Modeling of Molecular and Electron Kinetic Processes* (California, NRTC79-7R, 1979).
35. Belousov D.V., Golovin A.S., Gurashvili V.A., et al. Preprint IAE-5093/7 (Moscow, 1990).
36. Kochetov I.V., Kurnosov A.K., Loboyko A.I., et al. Preprint IAE-4014/12 (Moscow, 1984).
37. Elkin N.N., Kochetov I.V., Kurnosov A.K., Napartovich A.P. *J. Rus. Laser Res.*, **13**, 46 (1992).
38. Gear C.W. *Commun. Ass. Comput. Math.*, **14**, 185 (1971).
39. Golovin A.S., Gurashvili V.A., Kochetov I.V., et al. *Kvantovaya Elektron.*, **23**, 405 (1996) [*Quantum Electron.*, **26**, 395 (1996)].
40. Borodin A.M., Gurashvili V.A., Kuz'min V.N., et al. *Kvantovaya Elektron*., **23**, 315 (1996) [*Quantum Electron.*, **26**, 307 (1996)].
41. Golovin A.S., Gurashvili V.A., Kochetov I.V., et al. *Teplofiz. Vys. Temp*., **24**, 852 (1986) [*High Temp.*, **24**, 638 (1986)].